nature astronomy

LETTERS

PUBLISHED: 30 JANUARY 2017 | VOLUME: 1 | ARTICLE NUMBER: 0027

Origin of meteoritic stardust unveiled by a revised proton-capture rate of ^{17}O

M. Lugaro[1,2*], A. I. Karakas[2–4], C. G. Bruno[5], M. Aliotta[5], L. R. Nittler[6], D. Bemmerer[7], A. Best[8], A. Boeltzig[9], C. Broggini[10], A. Caciolli[11], F. Cavanna[12], G. F. Ciani[9], P. Corvisiero[12], T. Davinson[5], R. Depalo[11], A. Di Leva[8], Z. Elekes[13], F. Ferraro[12], A. Formicola[14], Zs. Fülöp[13], G. Gervino[15], A. Guglielmetti[16], C. Gustavino[17], Gy. Gyürky[13], G. Imbriani[8], M. Junker[14], R. Menegazzo[10], V. Mossa[18], F. R. Pantaleo[18], D. Piatti[11], P. Prati[12], D. A. Scott[5,†], O. Straniero[14,19], F. Strieder[20], T. Szücs[13], M. P. Takács[7] and D. Trezzi[16]

Stardust grains recovered from meteorites provide high-precision snapshots of the isotopic composition of the stellar environment in which they formed[1]. Attributing their origin to specific types of stars, however, often proves difficult. Intermediate-mass stars of 4–8 solar masses are expected to have contributed a large fraction of meteoritic stardust[2,3]. Yet, no grains have been found with the characteristic isotopic compositions expected for such stars[4,5]. This is a long-standing puzzle, which points to serious gaps in our understanding of the lifecycle of stars and dust in our Galaxy. Here we show that the increased proton-capture rate of ^{17}O reported by a recent underground experiment[6] leads to $^{17}O/^{16}O$ isotopic ratios that match those observed in a population of stardust grainsfor proton-burning temperatures of 60–80 MK. These temperatures are achieved at the base of the convective envelope during the late evolution of intermediate-mass stars of 4–8 solar masses[7–9], which reveals them as the most likely site of origin of the grains. This result provides direct evidence that these stars contributed to the dust inventory from which the Solar System formed.

Stardust grains found in meteorites (and also interplanetary dust particles and samples returned from the comet Wild 2) represent the very small fraction of presolar dust that survived destruction in the protosolar nebula. They originally condensed in the atmospheres of evolved stars and in nova and supernova ejecta and were preserved inside meteorites[1]. Their isotopic compositions are measured with high precision (a few percent uncertainty) via mass spectrometry and provide us with deep insights into stellar physics and the origin of elements and of dust in the Galaxy. Identified stardust includes both carbon-rich (diamond, graphite, silicon carbide) and oxygen-rich (for example, silicates and Al-rich oxides) grains, with carbon-rich grains condensing from gas where carbon atoms outnumber oxygen (C > O), and oxygen-rich grains from gas with C < O. Here we focus on oxide and silicate grains, which are classified into different groups mostly based on their oxygen isotopic compositions[10]. Group I grains make up the majority (~75%) of oxide and silicate grains and show excesses in ^{17}O characteristic of the first dredge-up in red giant stars of initial mass ~1–3 $M_{\odot}$, with a maximum $^{17}O/^{16}O$ ratio of ~0.003. Their origin is generally well understood and attributed to the O-rich phases of the subsequent asymptotic giant branch (AGB), where large amounts of dust condense in the cool, expanding stellar envelopes[2]. Group II grains represent roughly 10% of all presolar oxide grains, although this is a lower limit since measured compositions may suffer from isotopic dilution during ion probe analysis. Like Group I grains, they display excesses in ^{17}O ($^{17}O/^{16}O$ up to 0.0015), but are also highly depleted in ^{18}O, having $^{18}O/^{16}O$ ratios that are up to two orders of magnitude less than the corresponding value for the Sun. The initial ratio of the radioactive ^{26}Al (half life, $t_{1/2} = 0.7$ Myr) to ^{27}Al is inferred from ^{26}Mg excesses, and in Group II grains it reaches 0.1, almost an order of magnitude higher than the average ratio for Group I grains. While this composition is the indisputable signature of H burning activating proton captures on the oxygen isotopes and ^{25}Mg (the $^{25}Mg(p,\gamma)^{26}Al$ reaction), hypotheses on the site of formation for Group II grains are still tentative.

Hydrogen burning affects the surface composition of massive (>4 $M_{\odot}$) AGB stars when the base of the convective envelope becomes hot enough for proton-capture nucleosynthesis to occur[7]

[1]Konkoly Observatory, Research Centre for Astronomy and Earth Sciences, Hungarian Academy of Sciences, 1121 Budapest, Hungary. [2]Monash Centre for Astrophysics (MoCA), Monash University, Clayton, Victoria 3800, Australia. [3]Research School of Astronomy and Astrophysics, Australian National University, Canberra, Australian Capital Territory 2611, Australia. [4]Kavli Institute for the Physics and Mathematics of the Universe (WPI), University of Tokyo, Kashiwa, Chiba 277-8583, Japan. [5]SUPA, School of Physics and Astronomy, University of Edinburgh, Edinburgh EH9 3FD, UK. [6]Department of Terrestrial Magnetism, Carnegie Institution for Science, Washington DC 20015, USA. [7]Helmholtz-Zentrum Dresden-Rossendorf, Bautzner Landstrasse 400, 01328 Dresden, Germany. [8]Università di Napoli Federico II and INFN, Sezione di Napoli, Strada Comunale Cinthia, 80126 Napoli, Italy. [9]Gran Sasso Science Institute, INFN, Viale Francesco Crispi 7, 67100 L'Aquila, Italy. [10]INFN, Sezione di Padova, Via Francesco Marzolo 8, 35131 Padova, Italy. [11]Università degli Studi di Padova and INFN, Sezione di Padova, Via Francesco Marzolo 8, 35131 Padova, Italy. [12]Università degli Studi di Genova and INFN, Sezione di Genova, Via Dodecaneso 33, 16146 Genova, Italy. [13]Institute for Nuclear Research (MTA ATOMKI), PO Box 51, 4001 Debrecen, Hungary. [14]INFN, Laboratori Nazionali del Gran Sasso (LNGS), 67100 Assergi, Italy. [15]Università degli Studi di Torino and INFN, Sezione di Torino, Via Pietro Giuria 1, 10125 Torino, Italy. [16]Università degli Studi di Milano and INFN, Sezione di Milano, Via Giovanni Celoria 16, 20133 Milano, Italy. [17]INFN, Sezione di Roma La Sapienza, Piazzale Aldo Moro 2, 00185 Roma, Italy. [18]Università degli Studi di Bari and INFN, Sezione di Bari, Via Edoardo Orabona 4, 70125 Bari, Italy. [19]INAF, Osservatorio Astronomico di Teramo, 64100 Teramo, Italy. [20]South Dakota School of Mines, 501 East Saint Joseph Street, South Dakota 57701, USA. [†]Present address: Communications Audit UK, Aerotech Business Park, Bamfurlong Lane, Cheltenham GL51 6ST, UK. *e-mail: maria.lugaro@csfk.mta.hu

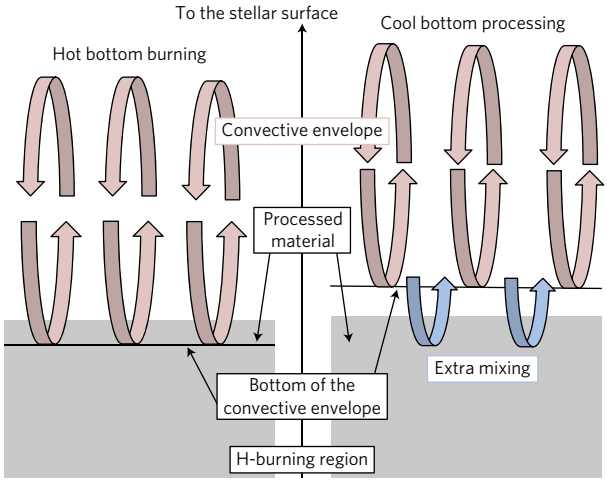

Figure 1 | Schematic of the internal structure of AGB stars at the interface between the H-burning region and the convective envelope. Hot bottom burning (left) and cool bottom processing (right) take place in massive and low-mass AGB stars, respectively, and carry material processed in the H-burning region to the stellar surface. The main differences between the two cases are that (1) material is processed at higher temperatures but lower densities in the case of HBB and (2) mixing occurs via convection in the case of HBB, whereas non-convective extra mixing needs to be invoked in the case of CBP.

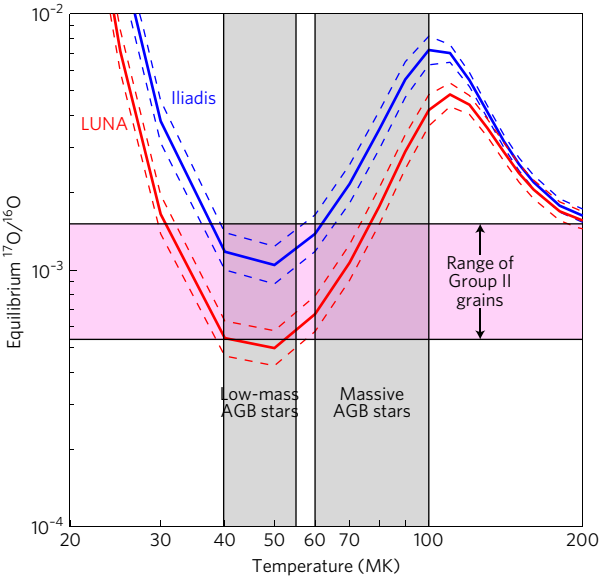

Figure 2 | Equilibrium $^{17}O/^{16}O$ ratio defined as the ratio of the production to destruction rates of ^{17}O in the temperature range of interest for AGB stars. We used the recommended (thick solid lines) and the lower and upper limits (thin dashed lines, essentially corresponding to the 1σ experimental uncertainty of the strength of the 64.5 keV resonance) of the $^{17}O(p, \alpha)^{14}N$ reaction rate from LUNA[6] and Iliadis *et al.*[12]. The horizontal pink band shows the range of $^{17}O/^{16}O$ values observed in Group II grains. The typical temperature ranges for CBP in low-mass AGB stars and for HBB in massive AGB stars are shown as grey vertical bands.

('hot bottom burning', HBB; Fig. 1). These are the brightest AGB stars, and the fact that they mostly show C/O < 1 is attributed to the operation of the carbon–nitrogen (CN) cycle, which depletes carbon[11]. In contrast, their less bright counterparts mostly show C/O > 1 as a result of the dredge-up of He-burning material rich in carbon. Characteristic temperatures of HBB exceed ~60 MK and, thanks to the fast convective turnover time (~1 yr), the composition of the whole envelope is quickly transmuted into the H-burning equilibrium abundances produced at the base of the envelope. Massive AGB stars are observed to generate significant amounts of dust, and based on current models of Galactic dust evolution, are expected to have contributed almost half of the O-rich dust of AGB origin in the Solar System[2,3]. However, no stardust grains have been found to show the signature of HBB because, although Group II grains show the highly depleted $^{18}O/^{16}O$ ratios qualitatively expected from HBB, their $^{17}O/^{16}O$ ratios are roughly two times lower than predicted[4,5] using the available reaction rates[12].

Currently, the preferred suggestion for the origin of Group II grains is that they formed in AGB stars of low mass (<1.5 $M_{\odot}$) that did not dredge-up enough carbon to become C-rich but experienced extra mixing below the bottom of the convective envelope ('cool bottom processing', CBP[13,14]; Fig. 1). In this scenario, material from the bottom of the convective envelope penetrates the thin radiative region located between the base of the convective envelope and the top of the H-burning shell, where the temperature and density increase steeply with mass depth and proton captures can occur (Fig. 1). While mechanisms have been proposed to explain the physical process driving this extra mixing[15], the current model of CBP is parametric: both the rate of the extra mixing and the depth reached are treated as free parameters, with the depth adjusted to reach temperatures in the range of 40–55 MK.

Whichever scenario we consider, the equilibrium $^{17}O/^{16}O$ ratio produced by H burning is determined by the competition between the processes that generate and destroy ^{17}O. Specifically, it depends on the ratio between the rate of the $^{16}O(p, \gamma)^{17}F$ reaction, which produces ^{17}O following the beta decay of ^{17}F ($t_{1/2}$ = 64 s), and the rate of the $^{17}O(p, \alpha)^{14}N$ reaction, which destroys ^{17}O. (Note that the $^{17}O(p, \gamma)^{18}F$ reaction rate is comparatively negligible at all temperatures considered here.) The $^{16}O(p, \gamma)^{17}F$ reaction rate is known to within 7%[5,12] and the $^{17}O(p, \alpha)^{14}N$ rate has recently been determined[6] from a direct measurement of the strength of the 64.5 keV resonance that dominates the reaction rate at temperatures between 10 and 100 MK[6] (the entire range of interest here). The experiment took place at the Laboratory for Underground Nuclear Astrophysics (LUNA) at Gran Sasso, Italy, where improved experimental procedures and a background for α-particle detection 15 times lower than in surface laboratories allowed for the most sensitive measurement to date[6]. The new rate is 2.0–2.5 times higher than previous evaluations[12,16]. At temperatures typical of CBP (40–55 MK), the new rate reproduces only the lowest $^{17}O/^{16}O$ values observed in Group II grains (Fig. 2). However, at 60–80 MK, the typical temperatures for HBB, the new rate reproduces most of the observed $^{17}O/^{16}O$ range, revealing the expected signature of HBB in stardust grains. HBB temperatures higher than ~80 MK are excluded for the parent stars of the grains.

Although the initial stellar mass and metallicity ranges at which HBB occurs as well as the AGB lifetime are model dependent[7–9], our result is robust because any massive AGB model experiencing HBB with temperatures between 60 and 80 MK will necessarily produce $^{17}O/^{16}O$ ratios in agreement with those observed in most Group II grains. Figure 3 shows the surface evolution of the oxygen isotopic ratios for three AGB models (of initial mass 4.5, 5.0 and 6.0 $M_{\odot}$ and solar metallicity) that experience HBB (see 'Methods'), compared with observed isotopic ratios for Group II stardust grains. The models evolve through the first and second dredge-ups at the end of core H and He burning, respectively, which increase the $^{17}O/^{16}O$ ratio by roughly a factor of five. During the subsequent AGB phase, HBB quickly (for example, for a 6.0 $M_{\odot}$ star, after about one-fifth of its total thermally pulsing AGB lifetime) shifts the oxygen isotopic composition to the equilibrium values corresponding to the burning temperature. Using the LUNA rate, the $^{17}O/^{16}O$ ratio produced

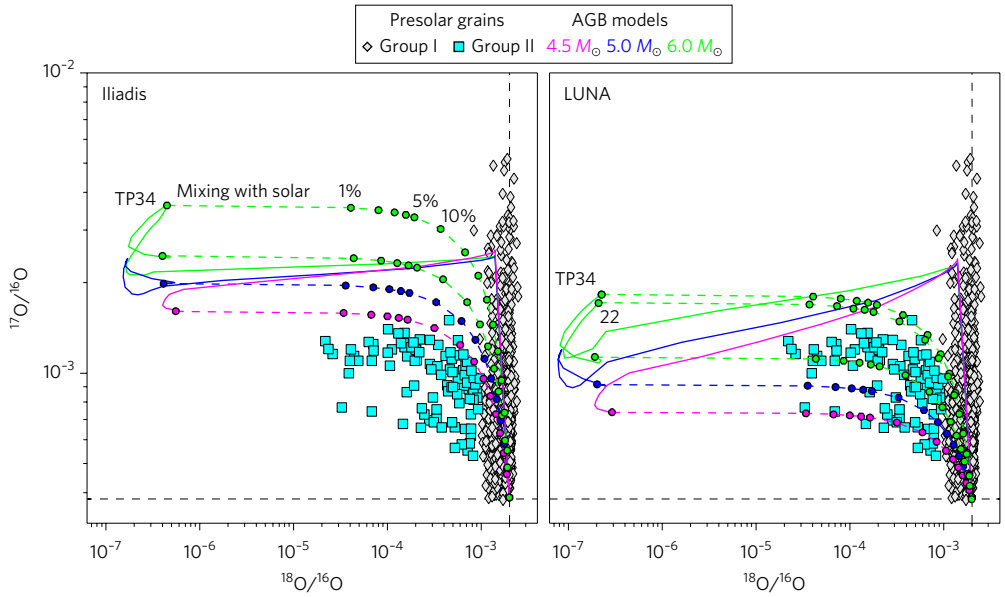

Figure 3 | Evolution of the oxygen isotopic ratios at the surface of AGB models of different masses. The evolutionary (solid) lines in the left and right panels were calculated using the old (Iliadis[12]) and new (LUNA[6]) $^{17}O(p,\alpha)^{14}N$ reaction rates, respectively. Uncertainties in either rate translates into changes in the $^{17}O/^{16}O$ ratio by at most 20%, that is, within the differences between the different stellar models. Isotopic ratios observed in Group II grains (filled square symbols[21] with error bars of 1σ, typically within the size of the symbol) cannot be reproduced by the old rate, regardless of the amount of dilution of AGB material with solar material (dotted lines), but are well reproduced with the new rate. The dilution is applied to the AGB composition at the end of the evolution for the three masses and, as examples, also at one-half and one-third of the AGB lifetime for the 6.0 $M_\odot$ star (labels TP34 and 22 indicate that the star evolved, respectively, through 34 and 22 thermal instabilities of the He shell out of the 53 computed in the models). Dashed vertical and horizontal lines indicate solar ratios for reference.

by HBB is roughly a factor of two lower than that obtained with the previous rate of Iliadis *et al.*[12]. The LUNA models nicely reproduce the oxygen ratios observed in Group II grains, when AGB material is diluted with material of solar composition. The dilution is required because HBB strongly depletes ^{18}O. This is in accordance with the non-detection of ^{18}O in bright O-rich AGB stars[17], but results in $^{18}O/^{16}O$ ratios more than two orders of magnitude lower than those observed in Group II grains. Dilution with solar material is particularly effective at increasing the $^{18}O/^{16}O$ ratio: for example, 99% of HBB material mixed with only 1% of solar material increases the $^{18}O/^{16}O$ ratio by two orders of magnitude. On the other hand, dilution has a comparatively minor effect on other isotopes measured in the grains because ^{17}O, ^{25}Mg and ^{26}Al are produced rather than destroyed in massive AGB stars. For example, it takes dilution with 50% of Solar System material to decrease the $^{17}O/^{16}O$ and $^{25}Mg/^{24}Mg$ ratios by a factor of two.

Dilution can be caused by percent-level traces of contaminant oxygen (for example, from terrestrial or non-presolar material) during isotopic measurements, which can result in $^{18}O/^{16}O$ up to $\sim10^{-4}$; however, laboratory contamination cannot easily explain grains with higher $^{18}O/^{16}O$ ratio values. For these, a dilution of the HBB signature composition with Solar System material at the level of up to a few tens of percent is required. Even higher dilution would result in a fraction of Group I grains also originating from massive AGB stars. Possible processes may involve dilution with previously ejected gas within the dust formation region; dilution with material in the interstellar medium; and/or a significantly lower value of the $^{18}O(p,\alpha)^{15}N$ reaction rate. A study of this reaction has recently been completed at LUNA and data analysis is in progress.

The other isotopic pairs measured in Group II grains are also consistent with an origin in massive AGB stars. The $^{25}Mg/^{24}Mg$ ratios are enhanced in massive AGB stars by the third dredge-up of material from the He inter-shell, where the $^{22}Ne(\alpha,n)^{25}Mg$ reaction is activated, and such a signature is seen in some presolar spinel ($MgAl_2O_4$) grains (Fig. 4a). Specifically, the value observed in a spinel grain named 14-12-7 (ref. [18]) (twice the $^{25}Mg/^{24}Mg$ ratio of the Sun) is close to that obtained in the final composition of the 5 $M_\odot$ model. However, grain OC2 (ref. [4]) and the majority of the other grains show a spread in the $^{25}Mg/^{24}Mg$ ratio from 1.0 to 1.5 times the solar value, that is, lower than predicted by the dilution computed using the final AGB composition. This may reflect partial equilibration of Mg isotopes in the grains themselves[19]. Alternatively, the lower $^{25}Mg/^{24}Mg$ ratios may be explained by truncating the AGB evolution to one-half or one-third of the total computed evolution (as illustrated in Figs. 3 and 4). This could result from a higher mass-loss rate and/or the effect of binary interactions. Another solution allowed within current model uncertainties is a third dredge-up that is less efficient than that calculated in our models. Finally, the high $^{26}Al/^{27}Al$ ratios typical of Group II grains (up to ~0.1) are also consistent with HBB (Fig. 4b), although an accurate analysis is currently hampered by the uncertainties in the ^{25}Mg and ^{26}Al proton-capture rates[12,20].

Our evidence that some meteoritic stardust grains exist whose O, Mg and Al isotopic composition is best accounted for by H-burning conditions characteristic of massive AGB stars proves that these stars were contributors of dust to the early Solar System. It further provides us with a new tool to deepen our understanding of uncertain physical processes in massive AGB stars, for which observational constraints are still scarce.

Methods

Stellar models. Stellar structure models with metallicities (Z) from half to double the solar Z (0.014; ref. [22]) were selected from the large set presented by Karakas[23] (computed with the Monash-Stromlo code[24]). No mass loss was assumed on the red giant branch and the Vassiliadis and Wood[25] mass-loss formulation was used on the AGB. The C-rich and N-rich low-temperature opacity tables were taken from Marigo & Aringer[26]. Convection was approximated using mixing length theory with a mixing-length parameter of 1.86 for all calculations. No convective overshoot was applied, although the algorithm

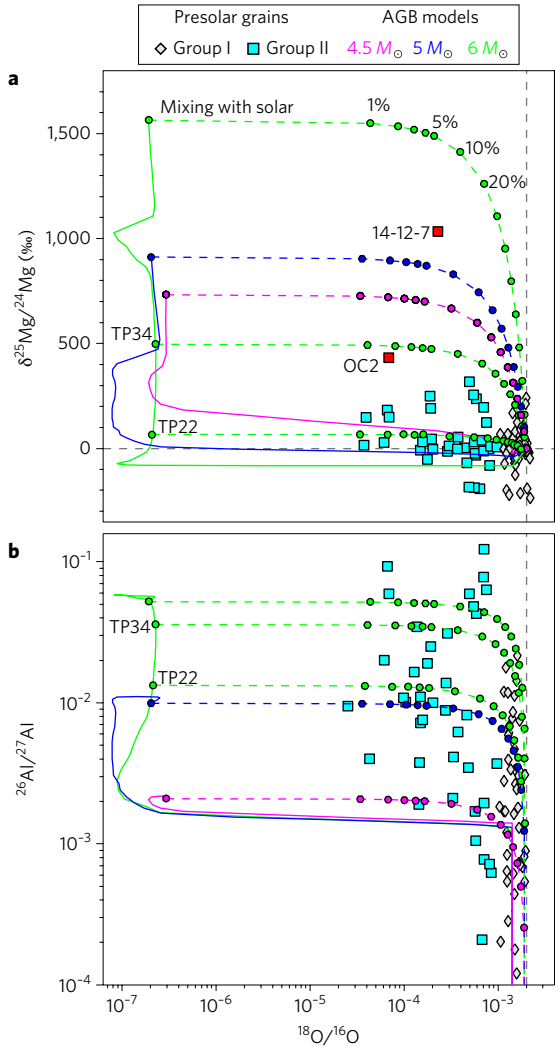

Figure 4 | Evolution of selected Mg versus O and Al versus O isotopic ratios at the surface of AGB models of different masses. Same as Fig. 3, with models calculated using the LUNA rate. **a**, Evolution of $\delta^{25}Mg/^{24}Mg$; values represent permil variations with respect to the Solar System value. The two spinel grains with excesses in ^{25}Mg (OC2 and 14-12-7) are highlighted in red. **b**, Evolution of the $^{26}Al/^{27}Al$ ratio.

described by Lattanzio[27] was used to search for a neutrally stable point for the border between convective and radiative zones.

From the previous study by Karakas[23], we selected some models with initial masses of 4.5–8.0 $M_\odot$ and canonical values for the He content; these are presented in Supplementary Table 1. More details on the physical quantities calculated from the models can be found in Table 1 of the Karakas's paper[23]. In Supplementary Table 1 we only report a summary of those that are most relevant here: the total number of thermal instabilities of the He-burning shell (thermal pulses, TPs); the maximum temperature at the base of the convective envelope (T_{bce}^{max}); the maximum temperature achieved in the inter-shell ($T_{inter\text{-}shell}^{max}$); and the mass lost during the whole evolution (M_{lost}^{total}). All the models experienced T_{bce}^{max} high enough to activate HBB, except for the 5.0 $M_\odot$ model with $Z=0.03$. It should be noted that the mass and metallicity ranges over which HBB occurs are model dependent: for the same mass and metallicity, models using more or less efficient convection (for example, via a different mixing length parameter or different mixing schemes) result in different temperatures[7,8]. All our stellar models also exhibited efficient third dredge-up, that is, C-rich material being carried from the He-rich inter-shell to the convective envelope. This is also model dependent. The possible TP-associated overshooting at the base of the convective region is not included in our models. In combination with the third dredge-up it would enrich the envelope with ^{16}O. However, this would not change the oxygen isotopic ratios at the stellar surface since HBB efficiently brings them to their equilibrium values, similar to the case of the carbon isotopic ratios. In the lower-mass stars where HBB is not activated, efficient third dredge-up of ^{16}O would be accompanied by efficient third dredge-up of ^{12}C, producing a C-rich envelope where the oxide and silicate grains considered here do not form.

Because of both the large dilution and the effect of HBB, most of the models lead to O-rich surfaces—the condition for formation of the oxide and silicate grains of interest here—during their whole evolution, except for the 4.5 $M_\odot$ model with $Z=0.014$ and the 5.0 $M_\odot$ model with $Z=0.007$. These exceptions become C-rich after the second last and last TP, respectively, which results in 40–50% of the ejected material being C-rich. For all the models, a relatively large fraction of the envelope material (20–30%) is still present when our calculations stopped converging. The abundances we calculated for the last model are either lower limits or a good approximation to the final enrichment, depending on possible further occurrence of third-dredge-up episodes beyond the point where our models stop converging.

We fed the computed stellar structure into the Monash post-processing code to calculate the detailed nucleosynthesis by simultaneously solving for the abundance changes brought about by nuclear reactions and by convection using a 'donor cell' advective scheme with two-stream (up and down) mixing. The simultaneous treatment of mixing and burning is required to model HBB in detail because the nuclear reactions may have timescales similar to or shorter than the mixing timescales, depending on where they occur in the envelope. In these cases it is not possible to make the assumption of instantaneous mixing at an average burning rate. Essentially our method couples mixing and burning together in the post processing to obtain the nucleosynthesis, while the energetic feedback of HBB is taken from the structure calculations performed using instantaneous mixing. The nucleosynthesis of elements up to Pb and Bi from the complete set of models from Karakas[23] with He canonical abundance can be found in Karakas & Lugaro[9], together with a full discussion of the results. Briefly, in models that experience HBB, T_{bce}^{max} is the main feature controlling the composition of the stellar surface, and specifically the oxygen and aluminium ratios that are measured in oxide and silicate stardust grains. In massive AGB stars of roughly solar metallicity, the Mg composition is affected mainly by the activation of the $^{22}Ne(\alpha, n)^{25}Mg$ and $^{22}Ne(\alpha, \gamma)^{26}Mg$ reactions in the He-rich inter-shell (where $T_{inter\text{-}shell}^{max}$ is well above the activation temperature of these reactions, ~300 MK, for all the models) and the subsequent third dredge-up of this material to the stellar surface. In comparison to this previous study[9], we updated the $^{22}Ne + \alpha$ and $^{25}Mg + \gamma$ reaction rates of Iliadis *et al.*[12] to those of Longland *et al.*[28] and Straniero *et al.*[20], respectively. Also, in the present study, we limited our calculations to a small network of 77 nuclear species, from neutrons to sulfur, plus the elements around the Fe peak, as described in Karakas[24]. This choice allowed us to run each model in a few hours and test different values of the $^{17}O(p, \alpha)^{14}N$ reaction rate: the recommended, the upper limit, and the lower limit from both Iliadis *et al.*[12] and LUNA[6]. For the $^{16}O(p, \gamma)^{17}F$ rate, we used the value recommended by Iliadis *et al.*[12], which has an uncertainty of 7%[5]. For the initial abundances, we used Asplund *et al.*[22] for the solar metallicity models, scaled down or up by factor of two for the $Z=0.007$ and $Z=0.03$ models, respectively. Although we calculated detailed predictions for all the models listed in Supplementary Table 1, for sake of clarity, we have restricted the content of our figures and discussion to the 4.5, 5.0 and 6.0 $M_\odot$ models with $Z=0.014$. Models with different metallicities in the same mass range have similar T_{bce}^{max} and provide similar results, except for the 5.0 $M_\odot$ model with $Z=0.03$, which does not exhibit HBB but remains O-rich due to the low efficiency of the third dredge-up combined with the high initial O abundance. On the other hand, in the 8.0 $M_\odot$ models, T_{bce}^{max} is too high to provide a match with the grain data (see Fig. 2). Stellar population synthesis models are needed to assess whether a number of Group I grains may also have originated from massive, super-solar-metallicity AGB stars that are O-rich and do not exhibit HBB.

Data availability. The data that support the plots within this paper and other findings of this study are available from the corresponding author on reasonable request.

Received 18 June 2016; accepted 5 December 2016; published 30 January 2017

References

1. Zinner, E. in *Treatise on Geochemistry* 2nd edn, Vol. 1 (ed. Davis, A. M.) 181–213 (Elsevier, 2014).
2. Gail, H.-P., Zhukovska, S. V., Hoppe, P. & Trieloff, M. Stardust from asymptotic giant branch stars. *Astrophys. J.* **698,** 1136–1154 (2009).
3. Zhukovska, S., Petrov, M. & Henning, T. Can star cluster environment affect dust input from massive AGB stars? *Astrophys. J.* **810,** 128 (2015).
4. Lugaro, M. *et al.* On the asymptotic giant branch star origin of peculiar spinel grain OC2. *Astron. Astrophys.* **461,** 657–664 (2007).
5. Iliadis, C., Angulo, C., Descouvemont, P., Lugaro, M. & Mohr, P. New reaction rate for $^{16}O(p,\gamma)^{17}F$ and its influence on the oxygen isotopic ratios in massive AGB stars. *Phys. Rev. C* **77,** 045802 (2008).
6. Bruno, C. G. *et al.* Improved direct measurement of the 64.5 keV resonance strength in the $^{17}O(p, \alpha)^{14}N$ reaction at LUNA. *Phys. Rev. Lett.* **117,** 142502 (2016).

7. Ventura, P., Di Criscienzo, M., Carini, R. & D'Antona, F. Yields of AGB and SAGB models with chemistry of low- and high-metallicity globular clusters. *Mon. Not. R. Astron. Soc.* **431,** 3642–3653 (2013).
8. Cristallo, S., Straniero, O., Piersanti, L. & Gobrecht, D. Evolution, nucleosynthesis, and yields of AGB stars at different metallicities. III. Intermediate-mass models, revised low-mass models, and the ph-FRUITY interface. *Astrophys. J. Suppl.* **219,** 40 (2015).
9. Karakas, A. I. & Lugaro, M. Stellar yields from metal-rich asymptotic giant branch models. *Astrophys. J.* **825,** 26 (2016).
10. Nittler, L. R., Alexander, C. M. O'D., Gao, X., Walker, R. M. & Zinner, E. Stellar sapphires: The properties and origins of presolar Al_2O_3 in meteorites. *Astrophys. J.* **483,** 475–495 (1997).
11. Wood, P. R., Bessell, M. S. & Fox, M. W. Long-period variables in the Magellanic Clouds: Supergiants, AGB stars, supernova precursors, planetary nebula precursors, and enrichment of the interstellar medium. *Astrophys. J.* **272,** 99–115 (1983).
12. Iliadis, C., Longland, R., Champagne, A. E., Coc, A. & Fitzgerald, R. Charged-particle thermonuclear reaction rates: II. Tables and graphs of reaction rates and probability density functions. *Nucl. Phys. A* **841,** 31–250 (2010).
13. Nollett, K. M., Busso, M. & Wasserburg, G. J. Cool bottom processes on the thermally pulsing asymptotic giant branch and the isotopic composition of circumstellar dust grains. *Astrophys. J.* **582,** 1036–1058 (2003).
14. Palmerini, S., La Cognata, M., Cristallo, S. & Busso, M. Deep mixing in evolved stars. I. The effect of reaction rate revisions from C to Al. *Astrophys. J.* **729,** 3 (2011).
15. Nucci, M. C. & Busso, M. Magnetohydrodynamics and deep mixing in evolved stars. I. two- and three-dimensional analytical models for the asymptotic giant branch. *Astrophys. J.* **787,** 141 (2014).
16. Buckner, M. Q. *et al.* High-intensity-beam study of $^{17}O(p,\gamma)^{18}F$ and thermonuclear reaction rates for ^{17}O+p. *Phys. Rev. C* **91,** 015812 (2015).
17. Justtanont, K. *et al.* Herschel observations of extreme OH/IR stars. The isotopic ratios of oxygen as a sign-post for the stellar mass. *Astron. Astrophys.* **578,** A115 (2015).
18. Gyngard, F. *et al.* Automated NanoSIMS measurements of spinel stardust from the Murray meteorite. *Astrophys. J.* **717,** 107–120 (2010).
19. Nittler, L. R. *et al.* Aluminum-, calcium- and titanium-rich oxide stardust in ordinary chondrite meteorites. *Astrophys. J.* **682,** 1450–1478 (2008).
20. Straniero, O. *et al.* Impact of a revised $^{25}Mg(p,\gamma)^{26}Al$ reaction rate on the operation of the Mg-Al cycle. *Astrophys. J.* **763,** 100 (2013).
21. Hynes, K. M. & Gyngard, F. In *40th Lunar and Planetary Science Conference* Abstract 1198 (Lunar and Planetary Institute, 2009); http://presolar.wustl.edu/~pgd/welcome.html
22. Asplund, M., Grevesse, N., Sauval, A. J. & Scott, P. The chemical composition of the Sun. *Ann. Rev. Astron. Astrophys.* **47,** 481–522 (2009).
23. Karakas, A. I. Helium enrichment and carbon-star production in metal-rich populations. *Mon. Not. R. Astron. Soc.* **445,** 347–358 (2014).
24. Karakas, A. I. Updated stellar yields from asymptotic giant branch models. *Mon. Not. R. Astron. Soc.* **403,** 1413–1425 (2010).
25. Vassiliadis, E. & Wood, P. R. Evolution of low- and intermediate-mass stars to the end of the asymptotic giant branch with mass loss. *Astrophys. J.* **413,** 641–657 (1993).
26. Marigo, P. & Aringer, B. Low-temperature gas opacity. ÆSOPUS: a versatile and quick computational tool. *Astron. Astrophys.* **508,** 1539–1569 (2009).
27. Lattanzio, J. C. The asymptotic giant branch evolution of 1.0–3.0 solar mass stars as a function of mass and composition. *Astrophys. J.* **311,** 708–730 (1986).
28. Longland, R., Iliadis, C. & Karakas, A. I. Reaction rates for the s-process neutron source $^{22}Ne + \alpha$. *Phys. Rev. C* **85,** 065809 (2012).

Acknowledgements

We thank O. Pols and R. Izzard for useful insights on binary systems and P. Marigo for discussion of our results. M.L. is a Momentum ('Lendület-2014' Programme) project leader of the Hungarian Academy of Sciences. M.L. and A.I.K. are grateful for the support of the National Computational Infrastructure National Facility at the Australian National University.

Author contributions

M.L. designed and carried out the research, ran the nucleosynthesis models, prepared the figures, and wrote the paper. A.I.K. ran the stellar structure models, discussed the results and wrote the paper. C.G.B. played a key role in the set up and running of the underground experiment relating to the $^{17}O(p,\alpha)^{14}N$ reaction and analysed the data to derive the new rate. M.A. contributed to running the experiment and wrote the paper. L.R.N. contributed to the collection of the stardust grain data, discussed the results, prepared the figures, and wrote the paper. The other authors are co-investigators who set up and ran the underground experiment that lasted about three years, from 2012 to 2015, and made the measurements possible. O.S. also discussed the results.

Additional information

Supplementary information is available for this paper.

Reprints and permissions information is available at www.nature.com/reprints.

Correspondence and requests for materials should be addressed to M.L.

How to cite this article: Lugaro, M. *et al.* Origin of meteoritic stardust unveiled by a revised proton-capture rate of ^{17}O. *Nat. Astron.* **1,** 0027 (2017).

Competing interests

The authors declare no competing financial interests.